PHYSICAL MODEL OF THE TROMBONE USING DYNAMIC GRIDS FOR FINITE DIFFERENCE SCHEMES

Silvin Willemsen

Multisensory Experience Lab
Aalborg University Copenhagen
Copenhagen, Denmark
`sil@create.aau.dk`

Stefan Bilbao, Michele Ducceschi

Acoustics and Audio Group
University of Edinburgh
Edinburgh, UK

Stefania Serafin

Multisensory Experience Lab
Aalborg University Copenhagen
Copenhagen, Denmark

ABSTRACT

The trombone...

1. INTRODUCTION

Intro intro
   Main challenge is to include time-varying length...

2. CONTINUOUS SYSTEM

Wave propagation in an acoustic tube can be approximated using a 1-dimensional model. Consider a tube of time-varying length $L = L(t)$ (in m) defined over spatial domain $x \in [0, L]$ and time $t \geq 0$. Using operators ∂_t and ∂_x denoting a first-order derivative with respect to time t and space x, respectively, a system of first-order PDEs describing the wave propagation in an acoustic tube can then be written as

$$\frac{S}{\rho_0 c^2}\partial_t p = -\partial_x(Sv) \tag{1a}$$

$$\rho_0 \partial_t v = -\partial_x p \tag{1b}$$

with pressure $p = p(x, t)$ (in N/m^2), particle velocity $v = v(x, t)$ (in m/s) and (circular) cross-sectional area $S(x)$ (in m^2). Furthermore, ρ_0 is the density of air (in kg/m^3) and c is the speed of sound in air (in m/s).

   Boundary conditions can then be imposed at the ends of domain, $x = 0, L$. We assume the left boundary (at the mouthpiece) to be closed and the right (at the bell) to be open according to

$$S(0, t)v(0, t) = 0, \quad \text{(Neumann, closed)} \tag{2a}$$

$$p(L, t) = 0. \quad \text{(Dirichlet, open)} \tag{2b}$$

In the following, these (lossless) boundary conditions will be modified to be coupled to a lip reed and radiating respectively.

2.1. Coupling to a Lip Reed

To excite the system, a lip reed can be modelled as a simple oscillating mass according to

$$M_r \frac{d^2 y}{dt^2} = -M_r \omega_0^2 y - M_r \sigma_r \frac{dy}{dt} + S_r \Delta p, \tag{3}$$

with displacement from the equilibrium $y = y(t)$, lip mass M_r (in kg), externally supplied (angular) frequency of oscillation $w_0 = w_0(t) = \sqrt{K/M_r}$ (in rad/s), stiffness $K = K(t)$ (in N/m), effective surface area S_r (in m^2) and

$$\Delta p = P_m - p(0, t) \tag{4}$$

is the difference between the pressure in the mouth P_m and the pressure in the mouth piece $p(0, t)$ (all in Pa). See Figure 1 for a schematic of the lip reed model. This pressure difference causes a volume flow velocity following the Bernoulli equation

$$U_B = w_r[y + H_0]_+ \text{sgn}(\Delta p)\sqrt{\frac{2|\Delta p|}{\rho_0}}, \tag{5}$$

(in m/s) with effective lip-reed width w_r (m), static equilibrium separation H_0 (in m) and $[\cdot]_+ = 0.5(\cdot + |\cdot|)$ describes the "positive part of". Notice that when $y + H_0 \leq 0$, the lips are closed and the volume velocity U_B is 0. Another volume flow is generated by the lip reed itself according to

$$U_r = S_r \frac{dy}{dt} \tag{6}$$

(in m/s). Assuming that the volume flow velocity is conserved, the total air volume entering the system is defined as

$$S(0)v(0, t) = U_B(t) + U_r(t). \tag{7}$$

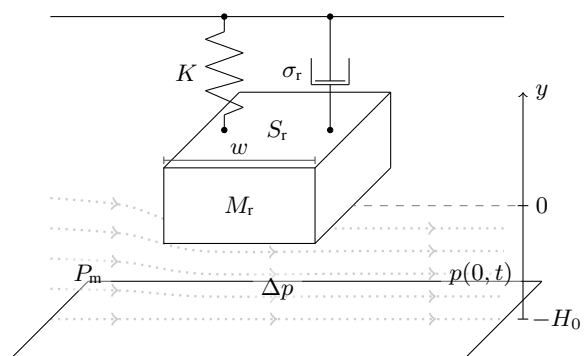The lip reed can then be coupled to the tube by modifying boundary condition (2a) to (7).

Figure 1: Lipsystem with the equilibrium at 0 and the distance from the lower lip H_0.

2.2. Radiation

As the bell-end of brass instruments is in a way "coupled" to the air, the tube loses energy at the bell, or right boundary. These losses can be modelled using a radiation model and lossless condition (2b) can be modified to be radiating instead. The radiation model used is the one for the unflanged cylindrical pipe proposed by Levine and Schwinger in [1] and discretised by Silva *et al.* in [2]. As this model is not important for the contribution of this work it will not be detailed here in full. The interested reader is instead referred to [3] for a comprehensive explanation.

3. DISCRETISATION

The continuous system described in the previous section is discretised using FDTD methods, which subdivide continuous equations into discrete points in space and time. Before moving on to this discretisation, we briefly introduce these methods along with several finite-difference operators.

3.1. Numerical Methods

Consider a 1D system described by state variable $u = u(x, t)$ with spatial domain $x \in \mathbb{R}$ and time $t \geq 0$. The spatial domain can be disctretised according to $x = lh$ with spatial index $l \in \mathbb{Z}$ and grid spacing h (in m) and time as $t = nk$ with temporal index $n \in \mathbb{Z}^{0+}$ and time step k (in s). Using these discrete variables state variable $u(x, t)$ can be discretised to grid function u_l^n.

Shift operators can then be applied to grid function u_l^n. Temporal and spatial shift operators are

$$e_{t+}u_l^n = u_l^{n+1}, \quad e_{t-}u_l^n = u_l^{n-1},$$
$$e_{x+}u_l^n = u_{l+1}^n, \quad e_{x-}u_l^n = u_{l-1}^n, \tag{8}$$

from which more complex operators can be derived. First-order derivatives can be approximated using forward, backward and centered difference operators in time

$$\delta_{t+} = \frac{e_{t+} - 1}{k}, \; \delta_{t-} = \frac{1 - e_{t-}}{k}, \; \delta_{t\cdot} = \frac{e_{t+} - e_{t-}}{2k}, \tag{9}$$

(all approximating ∂_t) and space

$$\delta_{x+} = \frac{e_{x+} - 1}{h}, \; \delta_{x-} = \frac{1 - e_{x-}}{h}, \; \delta_{x\cdot} = \frac{e_{x+} - e_{x-}}{2h}, \tag{10}$$

(all approximating ∂_x) where the identity operator 1 does not introduce any shift.

Furthermore, forward, backward and centered averaging operators can be defined in time

$$\mu_{t+} = \frac{e_{t+} + 1}{2}, \; \mu_{t-} = \frac{1 + e_{t-}}{2}, \; \mu_{t\cdot} = \frac{e_{t+} + e_{t-}}{2}, \tag{11}$$

and space

$$\mu_{x+} = \frac{e_{x+} + 1}{2}, \; \mu_{x-} = \frac{1 + e_{x-}}{2}, \; \mu_{x\cdot} = \frac{e_{x+} + e_{x-}}{2}. \tag{12}$$

Here, forward and backward averaging operators are extremely useful in the context of first-order systems as used in this paper. When applied to a grid function, the result may be interpreted as its value shifted by half a temporal or spatial step:

$$\mu_{t+}u_l^n = u_l^{n+1/2}, \quad \mu_{t-}u_l^n = u_l^{n-1/2}, \tag{13}$$
$$\mu_{x+}u_l^n = u_{l+1/2}^n, \quad \mu_{x-}u_l^n = u_{l-1/2}^n, \tag{14}$$

effectively placing the grid function on an *interleaved grid* which will be further elaborated on in the following.

3.2. Discrete Tube

We start discretising system (1) by placing velocity v on an interleaved grid, following [3], both in space and time. Domain $x \in [0, L]$ can be discretised to $l = [0, \ldots, N]$ where number of intervals between grid points is calculated using $N = \lfloor L/h \rfloor$.

The grid functions $p_l^n \approx p(x, t)$ and $v_{l+1/2}^{n+1/2} \approx v(x, t)$ (with reduced domain $l = [0, \ldots, N - 1]$) with $N + 1$ and N grid points respectively are then introduced along with discrete cross-sectional area $S_l \approx S(x)$ sampled at $x = lh$ to which the spatial operators defined in Section 3.1 can also be applied.

System (1) can then be discretised into the following system of finite difference schemes (FDSs)

$$\frac{\bar{S}_l}{\rho_0 c^2}\delta_{t+}p_l^n = -\delta_{x-}(S_{l+1/2}v_{l+1/2}^{n+1/2}), \tag{15a}$$

$$\rho_0\delta_{t-}v_{l+1/2}^{n+1/2} = -\delta_{x+}p_l^n, \tag{15b}$$

where $S_{l+1/2} = \mu_{x+}S_l$ and $\bar{S}_l = \mu_{x-}S_{l+1/2}$ are approximations to the continuous cross-sectional area $S(x)$. The values for $\bar{S}_l$ at the boundaries, i.e., $\bar{S}_0$ and $\bar{S}_N$ are set equal to $S(0)$ and $S(L)$.

Expanding the operators, we obtain the following recursion

$$p_l^{n+1} = p_l^n - \frac{\rho_0 c\lambda}{\bar{S}_l}(S_{l+1/2}v_{l+1/2}^{n+1/2} - S_{l-1/2}v_{l-1/2}^{n+1/2}), \tag{16a}$$

$$v_{l+1/2}^{n+1/2} = v_{l+1/2}^{n-1/2} - \frac{\lambda}{\rho_0 c}(p_{l+1}^n - p_l^n), \tag{16b}$$

where $\lambda = ck/h$ is referred to as the Courant number and

$$\lambda \leq 1 \tag{17}$$

in order for the scheme to be stable.

Finally, the boundary conditions in (2) can be discretised as

$$\mu_{x-}\left(S_{1/2}v_{1/2}^{n+1/2}\right) = 0 \tag{18a}$$
$$p_N^n = 0 \tag{18b}$$

3.3. Lip reed

As the lip reed interacts with the particle velocity of the tube, it is placed on the interleaved temporal grid, but kept on the regular spatial grid, as it interacts with the boundary at $l = 0$.

Equations (3) - (7) are discretised as follows:

$$M_r\delta_{tt}y^{n+1/2} = -M_r\omega_0^2\mu_{t\cdot}y^{n+1/2} - M_r\sigma_r\delta_{t\cdot}y^{n+1/2} + S_r\Delta p^{n+1/2} \tag{19a}$$

$$\Delta p^{n+1/2} = P_m - \mu_{t+}p_0^n \tag{19b}$$

$$U_B^{n+1/2} = w[y^{n+1/2} + H_0]_+\text{sgn}(\Delta p^{n+1/2}) \\ \cdot \sqrt{2|\Delta p^{n+1/2}|/\rho_0} \tag{19c}$$

$$U_r^{n+1/2} = S_r\delta_{t\cdot}y^{n+1/2} \tag{19d}$$

$$\mu_{x-}(S_{1/2}v_{1/2}^{n+1/2}) = U_B^{n+1/2} + U_r^{n+1/2} \tag{19e}$$

Boundary condition (18a) can be modified to Eq. (19e), effectively coupling the lip reed to the tube.
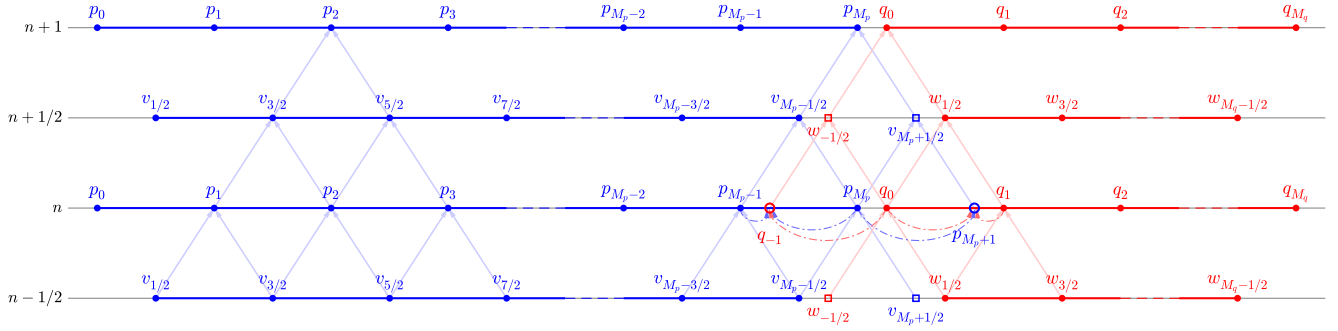
Figure 2: Schematic showing data flow of how different grid points at time index $n + 1$ are calculated. To prevent cluttering, arrows going straight up (indicating that the state of a grid point at time step n is needed to calculate the state of that grid point at $n + 1$) are suppressed. As an example of the usual case, the points required to calculate p_2^{n+1} are shown. Furthermore, the points needed to calculate $p_{M_p}^{n+1}$ and q_0^{n+1} are shown. The most important difference with the usual case is that the virtual grid points $p_{M_p+1}^n$ are the result of the interpolation of known pressure values at n

4. DYNAMIC GRID

Arguably the most characteristic feature of the trombone is its slide with which the length of the tube is altered and the resonating frequencies are changed. In a companion article [4], we present a method to dynamically change grid configurations of FDSs by adding and subtracting grid points based on paramters describing the system.

Though the paper shows changes in the wavespeed c rather than the length L, the effect of a change in either of these parameters has an identical effect on the system as long as the geometry is unchanged for the grid points.

We can split the FDS shown in (15) into two sets of first-order systems with lengths L_p and L_q. The pressure and particle velocity of the left system $p_{l_p}^n$ and $v_{l_p+1/2}^{n+1/2}$ are defined over discrete domains $l_p = [0, \ldots, M]$ and $l_p = [0, \ldots, M - 1]$ respectively. Here, $M = \lceil L_p/h \rceil$ where $\lceil \cdot \rceil$ denotes the ceiling operation. The pressure and particle velocity of the right system $q_{l_q}^n$ and $w_{l_q+1/2}^{n+1/2}$ are defined over discrete domains $l_q = [0, \ldots, M_q]$ and $l_q = [0, \ldots, M_q - 1]$ respectively. Here $M_q = \lfloor L_q/h \rfloor$ where $\lfloor \cdot \rfloor$ denotes the flooring operation. The resulting system then becomes

$$\frac{\bar{S}_l}{\rho_0 c^2}\delta_{t+}p_{l_p}^n = -\delta_{x-}(S_{l+1/2}v_{l_p+1/2}^{n+1/2}), \tag{20a}$$

$$\rho_0\delta_{t-}v_{l_p+1/2}^{n+1/2} = -\delta_{x+}p_{l_p}^n, \tag{20b}$$

$$\frac{\bar{S}_l}{\rho_0 c^2}\delta_{t+}q_{l_q}^n = -\delta_{x-}(S_{l+1/2}w_{l_q+1/2}^{n+1/2}), \tag{20c}$$

$$\rho_0\delta_{t-}w_{l_q+1/2}^{n+1/2} = -\delta_{x+}q_{l_q}^n, \tag{20d}$$

The outer boundaries of the system ($l_p = 0$ and $l_q = M_q$) are the same as for the full system. The inner boundaries ($l_p = M_p$ and $l_q = 0$), however, are connected according to the method described in [4].

A visual of the calculations used at the connection location of the two schemes can be found in Figure 2.

One can change the

As the geometry varies it matters a lot where points are added and subtracted.

Part of tube	Length (cm)	Radius (cm)
Inner slide (1)	70.8	0.69
Outer slide (extended) (2)	53	0.72
Slide crook (3)	17.7	0.74
Outer slide (extended) (4)	53	0.72
Inner slide (5)	71.1	0.69
Gooseneck (6)	24.1	0.71
Tuning slide (7)	25.4	0.75, 1.07
Bell flare (8)	56.7 ←check	1, 10.8

Table 1: Geometry of a measured trombone taken from [5]. Numbers correspond to Figure 3.

4.1. Adding and removing grid points

Use average to prevent drift when $\alpha = 0$ and stays 0.

The main challenge, though, is to apply the method to a system of first-order equations rather than the second-order 1D wave equation presented in [4]. Rather than adding points to the left and right system in alternating fashion, points are added to pressures p and q and velocities v and w respectively

5. IMPLEMENTATION
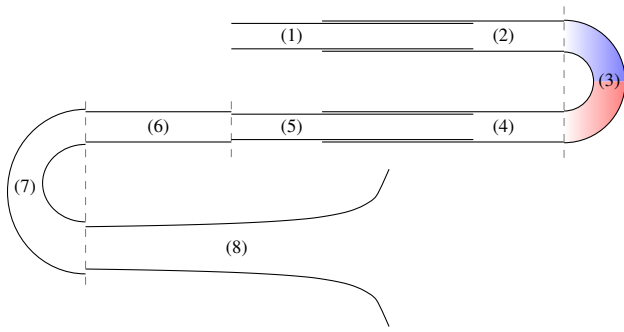
5.1. Parameters

A schematic showing the trombone geometry is shown in Figure 3 and the lengths and radii used in Table 1.

Other parameters used in the simulation can be found in Table 2.

5.2. Order of Calculation

6. CONCLUSION AND FUTURE WORK

Investigate the possibility of adding / removing grid points at points where the cross-sectional area is varying.

Figure 3: Schematic of the trombone. Numbers correspond to the parts of the tube found in Table 1 and dashed lines highlight where parts are separated. The scheme is split in the middle of the slide crook with the colours corresponding to those in 2.

Name	Symbol (unit)	Value
Tube		
Length	L (m)	$2.685 \leq L \leq 3.718^{\star}$
Air density	ρ_0 (kg/m^3)	1.1769**
Wave speed	c (m/s)	347.23**
Geometry	S (m^2)	See Table 1.
Lip reed		
Mass	M_r (kg)	$5.37 \cdot 10^{-5}$*
Frequency	ω_0 (rad/s)	$?? \leq \omega_0 \leq ??$
Mouth pressure	P_m (Pa)	$0 \leq P_m \leq 6000??$
Damping	σ_r (s^{-1})	5*
Eff. surface area	S_r (m^2)	$1.46 \cdot 10^{-5}$*
Width	w_r (m)	0.01*
Equilibrium	H_0 (m)	$2.9 \cdot 10^{-4}$*

Table 2: List of parameter values used for the simulation. Taken from *[5], *[3] or **[6] with temperature $T = 26.85°C$.

7. REFERENCES

[1] H. Levine and J. Schwinger, "On the radiation of sound from an unflanged circular pipe," *Physical Review*, vol. 73, no. 2, pp. 383–406, 1948.

[2] F. Silva, P. Guillemain, J. Kergomard, B. Mallaroni, and A. Norris, "Approximation formulae for the acoustic radiation impedance of a cylindrical pipe," *Journal of Sound and Vibration*, vol. 322, pp. 255–263, 2009.

[3] R. L. Harrison-Harsley, *Physical Modelling of Brass Instruments using Finite-Difference Time-Domain Methods*, Ph.D. thesis, University of Edinburgh, 2018.

[4] S. Willemsen, S. Bilbao, M. Ducceschi, and S. Serafin, "Dynamic grids for finite-difference schemes in musical instrument simulations," in *Proc. of the 23rd Int. Conf. on Digital Audio Effects (DAFx)*, 2021.

[5] T. Smyth and F. S. Scott, "Trombone synthesis by model and measurement," *EURASIP Journal on Advances in Signal Processing*, 2011.

[6] A. H. Benade, "On the propagation of sound waves in a cylindrical conduit," *Journal of the Acoustical Society of America*, vol. 44, no. 2, pp. 616–623, 1968.

[7] JUCE, "JUCE," Available at https://juce.com/, accessed March 21, 2021.